Open-File Report

Site Characterization for Stations 6 & 7, El Centro Strong Motion Array, Imperial Valley, California

A. T. F. Chen

M. J. Bennett

U.S. Geological Survey

Menlo Park, California 94025

Open-File Report 82-1040

August, 1982

TABLE OF CONTENTS

ILLUSTRATIONS

TABLES

INTRODUCTION

The Imperial Valley earthquake of October 15, 1979 triggered no less than 30 accelerographs within 100 km of the epicenter and produced many valuable close-in strong-motion records. The earthquake also generated a 1.7g vertical acceleration reading which is the largest ground-motion acceleration ever measured.

It is not by accident that there were so many accelerograph stations in the close-in region of the earthquake. Both the El Centro strong motion array and the El Centro differential motion array were installed with specific types of studies in mind. The strong motion array was installed to collect close-in strong motion records and the differential motion array was designed to study the effect of seismic wave on long structures. That the earthquake occurred after both arrays had been installed and operational makes the earthquake itself even more scientifically significant.

Because of the scientific significance of the earthquake ground motions, additional field studies were conducted to attain a better understanding of the local, near surface geology of the strong motion station sites. Geologic, geotechnical, and geophysical profiles were made at the strong motion stations to determine the stratigraphy and seismic characteristics of the sediments. We used cone penetration tests, samples and the drillers logs to define the stratigraphy and a down-hole seismic survey to make shear wave velocity profiles. The locations of the seismic stations are shown in figure 1.

The ground motion data from the earthquake indicate that the variation in peak surface acceleration cannot be solely attributed to the radiation pattern (Muller and others, 1982). The effect of local geology is also believed to have played an important role. To analyze the effect of local geology at the accelerograph station, certain engineering properties of the surficial

deposits at that station need to be assessed and ground motion analyses need to be made. Under intense seismic shaking, most soils exhibit nonlinear behavior of which the degree of nonlinearity is primarily dictated by their shear strength. Consequently, in addition to the traditional shear modulus needed for elastic analysis, the soil properties needed for nonlinear analyses should also include the shear strength.

This report characterizes the sediments at stations 6 and 7 of the El Centro strong motion array. We present our best estimates of the shear modulus vs. depth and shear strength vs. depth profiles. These profiles are estimated from available field data (wave velocity profiles and cone penetration records), regional geology, limited laboratory data, and a number of engineering correlations. We limited our investigation to stations 6 and 7 because wave velocity profiles from these stations were the only ones available at the time of this study.

REGIONAL AND LOCAL GEOLOGY

The Imperial Valley is located in southern California in the Salton trough geomorphic province (fig. 2). The Salton trough is over 1,000 km long and includes the Coachella and Imperial Valleys in California and the Mexicali Valley and Gulf of California in Mexico. The terrestrial portion of the trough has a natural divide created by the delta of the Colorado River. The Imperial Valley north of the delta has been cut off from the rest of the trough by the delta and subsequently has turned into a closed basin with internal drainage. The central part of the Imperial Valley contains the Salton Sea at an elevation of 70 m below sea level. Today, the part of the trough occupied by the Imperial Valley is sinking at a rate of 3.5 cm per year relative to the surrounding mountains (Elders, 1979).

The Gulf of California, including the Salton Trough, began opening during the Pliocene or Miocene. The late Tertiary-early Quaternary sediments that have filled the trough consist of alluvial fan boulder gravel, sandy and silty flood plain sediment, and lacustrine and marine silts and clays. Marine environments range from brackish to full marine conditions. In the mid-Pliestocene the Colorado River created a delta across the basin near Yuma, Arizona. The delta isolated the Imperial Valley from the southern part of the trough. The depositional history of the Imperial Valley was significantly changed by this event. Marine conditons were replaced by alternating continental valley fill and lacustrine deposits. Total sediment thickness in the center of the Imperial Valley is between 6 and 7 km (Elders, 1979). Most of this sediment may have accumulated in Quaternary time (Sharp, 1972). The Imperial Valley has been the site of numerous lakes created by channel shifts of the Colorado River. The river naturally moves its distributary channels during flood stage. Between 300 and 1600 years ago natural flooding from the Colorado River filled the Imperial Valley and created Lake Cahuilla (Van De Kamp, 1973, p. 829). The present Salton Sea was created in 1905 by man induced flooding from the Colorado River (Mendenhall, 1909). The lake that was created has remained relatively stable because of continued run-off from irrigation water.

The sediments within the basin are folded and faulted with these processes continuing at the present time (Sharp, 1972, and Elders, 1979). Folded layers of older sediment can be seen along the margins of the trough. Younger sediments show the effects of erosional truncations caused by recent warping. Folding is most pronounced in sediment bordering faults or bounded by faults (Sharp, 1972).

Major bounding faults in the Imperial Valley include the San Andreas, San Jacinto and Elsinore fault zones. The Imperial and Brawley fault zones are located in the center of the valley. The relationship between the major fault zones and those in the center of the valley are uncertain. Except for the Brawley fault all of the above named faults show San Andreas type characteristics such as, linearity, northwest-southeast trend, right lateral offset, and evidence of recent activity. The Brawley and Imperial faults bound an area called the Mesquite depression. The depression is being formed as a result of right lateral offset along the faults and pull-apart between the faults.

Strong motion stations 6 and 7 are located in a portion of the valley underlain by a veneer of Lake Cahuilla clay and beds of sand from channels and the Colorado River delta (Van De Kamp, 1972). Subsurface correlation of sediment in this area is difficult because of rapid changes in thickness and lithology. Fine-grained lacustrine deposits are cut by channels and filled with fine sand or clayey silt depending on the method of filling. The generalized geology of the study area is shown in figure 3.

Stations 6 and 7 are about 2 kms apart and lie on opposite sides of the Imperial fault (fig. 1). Station 6 is located between the Imperial and Brawley faults within the Mesquite depression at an elevation of -30 m. Station 7 lies to the west of the Mesquite depression at an elevation of -20 m. Both stations are located on the clay facies part of Lake Cahuilla (Van De Kamp, 1972). Sand beds within the clay facies were deposited in channels that meandered across the lake bottom surface during low water stands.

The New River and the Alamo River provide the principle means of transporting sediment in the valley today, but in the recent past many small distributaries also transported sediment within the valley. Van De Kamp

(1972) shows several buried channels associated with the Mesquite depression. Youd and Wieczorek (1982) describe a 11-km-long relict channel that runs from the Mexican border to just south of Holtville. Channels such as this channel provide the numerous discontinuous sand beds within the lacustrine sediment.

Stations 6 and 7 are located in areas with different tectonic conditions even though they are only 2 km apart. Station 6 is located between the Imperial and Brawley faults and is moving downward relative to station 7 which is on the west side of the Imperial fault.

FIELD PROCEDURES

The first step in the field investigation was to profile the sediment using the cone penetration test (CPT). These tests were made by Ertec Western, Inc., Long Beach, California, under purchase order numbers 54556 and 54560. The CPT profiles were used to determine soil types and bed thickness. The profiles were also used to select sampling intervals. The second part of the field investigation involved drilling holes for sampling and for placing casing to be used for seismic measurements. Samples were taken using thin-walled tubes and split spoons. The split spoon sampling method also provides estimates of soil density. After profiling and sampling were completed down-hole P- and S-wave velocity measurements were made.

Cone penetration test. The cone penetration test (ASTM D 3441-75T) measures the forces required to push a cone into the sediment. The cone contains strain gauges at the tip and above the tip that measure soil resistance at the tip (q_c) and the soil friction on a sleeve above the tip (f_s). The ratio between side friction and tip resistance, expressed as percent, is termed the friction ratio (R_f). These three measures of cone

penetration resistance were used to construct profiles at sites 6 and 7 (figs. 4 and 5). The tip resistance was used to estimate relative density using fig. 6. Shear strength of clays was estimated from cone records by taking 80 % of f_s as reconnended by Drnevich and others (1974). With the limited sampling done the CPT became the prime indicator of sediment type. Sediment type is shown in the log in figs. 4 and 5. Sediment type was interpreted from the relations between tip resistance and friction ratio. Coarse-grained sediment has low friction ratios (less than 2) whereas fine-grained sediment has higher ratios (greater than 4). Classifications using tip resistance and friction ratio have been developed by Sanglerat (1972), Schmertmann (1978), and Martin and Douglas (1981). The advantage of the CPT is that a continuous recording of tip resistance and friction ratio is made from which sediment type and strength can be interpreted.

Sampling. Samples were obtained using a truck-mounted drill rig that drilled 12-cm diameter holes to 76 m. The CPT profiles were used to select sampling intervals. Two methods of sampling were used. One sampling method used thin-walled tubes of 5-cm and 7.6-cm diameter. The other sampling method used thick-walled split-spoons of 3.5-cm diameter. Split-spoons are the sampling tool of the standard penetration test (SPT). In the SPT (ASTM D 1586-67T), split-spoon samplers are driven into the sediment by dropping a 63.5 kg hammer 76 cm. The number of blows, N, to advance the sampler 30 cm is a measure of the sediment strength or relative density (Terzaghi and Peck, 1967). The penetration resistance measured by the SPT was used with the CPT data to classify the sediment according to density. Samples from the SPT were placed in plastic bags, tube samples were capped and eventually stored in a high humidity room. The types and depths of samples are listed below.

Hole & unit no.	depth (m)	sample type
6-1	2.4-2.9	SPT
6-1	2.4-3.0	5-cm tube
6-1	3.0-3.7	5-cm tube
6-1	6.1-6.9	7.6-cm tube
6-2	11.3-11.7	SPT
6-2	13.7-14.5	7.6-cm tube
6-3	21.3-22.1	7.6-cm tube
6-5	28.7-29.1	SPT
7-1	2.4-2.9	SPT
7-2	13.7-14.5	7.6-cm tube
7-3	22.6-23.0	SPT
7-3	26.5-26.7	SPT

After sampling the holes were cased with 7.6-cm diameter PVC tubing to keep the hole open and provide a uniform and stable surface for the seismic probe.

Seismic Recording. Seismic waves were generated and recorded using the technique introduced by Kobayashi (1959), discussed by Warrick (1974), and used by Fumal and others (1982). Compression and shear waves were generated by striking an "anvil" with a hammer. Compression waves (P-waves) are generated by vertically striking a steel plate on the ground. Shear waves (S-waves) were generated by striking the end of a large horizontal timber held firmly on the ground by the wheels of a truck. The timing signal for the recordings, in both cases, is generated by the metal hammer striking the anvil. The generated seismic waves were monitored by a down hole geophone. The geophone was moved in 2.5-m increments for testing and locked in place by an inflatable diaphram. Seismic wave measurements were recorded on photographic paper by an oscillograph.

LABORATORY PROCEDURES

Samples were tested to classify sediment for descriptive purposes and to investigate physical properties such as strength, grain size, and bulk density. Capped tube samples were extruded in the laboratory and stored

vertically in a high-humidity room along with bag samples from the SPT. Strength tests were made only on tube samples. Testing procedures followed ASTM recommendations, tests included:

Density. Bulk density measurements were made from undisturbed tube samples. Length of samples ranged from 7.5 cm to 12 cm, diameter of samples averaged 5.1 cm and 7.6 cm. After the sample ends were trimmed length and diameter were determined from the average of 3 measurements. Samples were weighed to the nearest 0.1 gm and returned to the humidity room or used for strength tests. Bulk density was used to calculate effective stress.

Grain size. Grain size was determined using procedures outlined in ASTM D 422-63. Boundaries for size classes are 2 mm, gravel-sand; 0.062 mm, sand-silt; and 0.004 mm for silt-clay. Grain size greater than 0.062 mm was determined by sieving, grain size less than 0.062 mm was determined by hydrometer. Size distribution curves were used to determine sorting and median grain size. Sediment was classified according to the unified soil classification (fig. 7) (ASTM D 2487-69). Sediment names such as silty sand and clayey silt were based on the classification of Shepard (1954) (fig. 8).

Atterberg limits. The liquid and plastic limits represent the water content at the boundaries between the liquid and plastic states and the plastic and solid states, respectivly. The limits are a part of the unified soil classification. Further discussion of the limits is found in Lambe and Whitman (1969), Seed and others (1964), and Casagrande (1948). We followed ASTM procedures D 423-66 and D 424-59 in determining the liquid and plastic limits.

The natural water content is the ratio, expressed as percent, between the weight of free water and the weight of solid particles in sediment. Samples were weighed, dried overnight in an oven at 110^{o} C (ASTM D 2216-80) and

reweighed to determined the amount of water loss. The relationship between the natural water content and the liquid and plastic limits is expressed as the liquidity index. This index is the ratio of the difference of the natural water content and the plastic limit to the difference between the liquid and plastic limits. The liquidity index defines the physical state of the sediment and serves as a means of estimating the state of consolidation (Skempton, 1944).

Strength. Sediment strength is used in ground responce calculations that are discussed later on under the heading SHEAR STRENGTH PROFILES. Sediment strength was measured in the laboratory by a hand-operated vane shear device and by unconfined compression tests. The vane shear device was used to determine the shear strength of tube samples by rotating the top of the vane at a rate of 90^{o} per minute. The dimension of the vane is 1.2 cm by 1.2 cm. Unconfined compressive strength was determined on samples with a length to diameter ratio between 2 and 3. Tests were run at axial strains between 0.5 and 2.0% per minute (ASTM D 2166-66). Sediment strength was also interpreted from CPT data.

SITE DESCRIPTION

Sediment characteristics. The fine-grained sediments are classified by the unified soil classification shown in fig. 7. The Shepard classification used to the name the sediments is shown in fig. 8. Test results and descriptions are listed in tables 1, 2, and 3. Profiles and interpreted logs are shown in figs. 4 and 5.

The test results show two general types of sediment. Type 1 is comprised of very dense very fine sand and silt and is referred to as "sandy". The upper contacts of the sandy beds are usually sharp, lower contacts are both

sharp and transitional. We believe the sandy beds are channel deposits, called "shoestring sands" by Van De Kamp (1973).

Type 2 is comprised of reddish brown stiff to very stiff clayey silts to silty clay and is referred to as "clayey". The clayey sediment generally contains less than 7% sand, rare gastropods, rare to common gypsum nodules, and fine sandy to silty laminations. The liquidity index of the clayey sediments ranges between +0.2 and -0.2. The low index is typical of deeply buried or desiccated sediment. Because of the relatively shallow depth of the samples descication is probably the cause of the low liquidity index. These characteristics indicate that the clayey sediment is lacustrine.

Effective stress. The effective overburden pressure (σ'_v) plays an important role in the interpretation of cone penetration records for geotechnical parameters. This vertical effective stress in turn is controlled by the bulk density of individual soil layers and the local hydrological condition. In most cases, unrealistic estimates of σ'_v are caused by erroneous assessment of the ground water condition.

The down-hole P-wave survey at both stations indicates that the ground water table is near the surface at station 7 and at the lithological interface 8 meters below the surface at station 6 (Muller and others, 1982). Drilling records at station 6 show that the water-bearing sand layer immediately below that interface is under artesian pressure (Porcella, private communication). Water eventually seeped to the surface but no blowout or other difficulties was experienced during drilling.

Laboratory determination of bulk (wet) density of cohesive sediment from these stations were few and were limited to sediment at relatively shallow depths. Bulk densities for other soil deposits were assigned as 2.0 or 2.1 gm/cc depending on the cone resistance and driller's description of each

deposit. The estimated values of bulk densities at each station are shown in tables 2 and 3.

The vertical effective stress profiles computed from bulk density estimates and available ground water table information are shown in figure 9. We have assumed that the ground water table is at the surface at station 7 and 8 meters below the surface with an artesian pressure head that reaches to the surface at station 6. In assuming the artesian pressure head, we not only considered the fact that water did reach the surface with no evidence of high pressure to cause blowout or collapse of the drill hole, but also found that this estimate of artesian pressure is consistent with the shear strength-effective stress ratio for the silty clay layer at 15-25 meters depth, as will be discussed further later in the report.

One other factor that plays a major role in assessing getechnical parameters is the past loading history which is often expressed in terms of the overconsolidation ratio, OCR. Consideration of the regional geology led us to believe that overconsolidation due to an excessive amount of surface erosion at these two stations is unlikely. Overconsolidation then is caused either by dessication or lowering of ground water table. Desiccation would only limit the overconsolidation to near surface cohesive sediments whereas change of ground water table can only provide slight increase to the OCR. Consequently, deeper deposits at these two stations are expected to be normally consolidated to slightly overconsolidated.

SHEAR MODULUS PROFILES

For most soils, shear modulus is a strain-dependent property; its value decreases with the increasing strain amplitude. In down-hole seismic velocity measurements, only a limited amount of energy is generated at the ground

surface. As a result, the amplitude of the recorded particle velocities is generally very low. The shear strain amplitudes associated with these low velocity amplitudes are mostly at the 10^{-4} percent level. Consequently, the shear modulus values derived from down-hole measurements are accepted as G_{max}, the low-strain shear modulus, or the initial tangent shear modulus.

Shear modulus is related to the shear wave velocity, v_s by:

$$G = \rho v_s^2 \qquad (1)$$

in which ρ is the mass density. Based on the information given in tables 2 and 3, the shear modulus versus depth profiles were computed using eq. (1) and are shown in figures 10 and 11.

It should be noted that the velocities obtained from the down-hole survey represent the average value over a fixed interval. It follows that G_{max} shown in figures 8 and 9 should also be considered as average values over an interval which is 2.5 m for this investigation.

The slight shifts in G_{max} values in figures 10 and 11 are due to changes in density and may be ignored. Comparison between the same two figures shows that the sediment between 20 and 70 m (67 and 233 ft) at station 7 is stiffer than sediment at an equal depth at station 6. In addition, layers of alterating stiffness exist at station 6 whereas the stiffness increases monotonically with depth at station 7.

SHEAR STRENGTH PROFILES

As a general rule, the shear strength of a sediment in situ is a function of the effective overburden pressure, the void ratio, and the past loading history. There are many measures of shear strength with respect to sediment

type, drainage condition and loading path. For one-dimensional seismic response analysis of a horizontally layered system where shear wave motion dominates, the measure for shear strength is the maximum applied shear stress, τ_{max}, which is simply the maximum shear stress a soil element can sustain on its vertical or horizontal plane (Hardin and Drnevich, 1972). For both cohesive and cohesionless sediments under earthquake loading, τ_{max} can be computed from an equation given by Hardin and Drnevich (1972):

$$\tau_{max} = \left\{ \left[\frac{(1+K_o)}{2} \sigma_v' \sin\phi' + c\cos\phi' \right]^2 - \left[\frac{(1-K_o)}{2} \sigma_v' \right]^2 \right\}^{\frac{1}{2}} \qquad (2)$$

in which K_0 = coefficient of lateral stress at rest; σ' = vertical effective stress, c is the cohesion intercept, and ϕ' is the drained angle of friction.

Existing field procedures do not allow direct conversion from cone penetration data to individual parameters K_0, c, and ϕ' and therefore, a direct application of Eq. (2) is not possible. For cohesive sediments such as silt, clay, or the combination, the CPT results lead to a gross estimate of the undrained shear strength, S_u. For cohesionless sediments, the CPT results can lead to a reasonable estimate of ϕ', and the possible use of Eq. (2). However, we failed to find any means of estimating any measure of shear strength from CPT data for marginally cohesive sediments such as silty sand or sandy silt. The procedure used for estimating the shear strength of cohesive and cohesionless sediments is briefly described below.

First, to estimate S_u for cohesive sediment, we use the relation proposed by Drnevich and others (1974):

$$S_u = 0.8 * f_s \qquad (3)$$

where f_s is the sleeve friction resistance registered by the cone. This equation was based on results of cone penetration testing and triaxial testing performed on undisturbed samples of a variety of cohesive soils that include residual silty clays, compacted embankments, and clayey silts. The unconfined compression tests we conducted showed that S_u=0.9 kg/cm^2 for soil layer 6-1 whereas Eq. (3) yields S_u=0.8 kg/cm^2. We thus believe that Eq. (3) is capable of predicting S_u with adequate accuracy.

The ratio of S_u of a sediment to its overburden effective stress, S_u/σ_v' reflects the state of overconsolidation of that sediment. Assuming S_u/σ_v' =0.33 for normally consolidated clays and using the empirical relation as shown in figure 10 (Schmertmann, 1978), we can determine the overconsolidation ratio, OCR, for a particular cohesive layer.

We further assume that cohesionless sediment immediately below a cohesive sediment has the same OCR as that cohesive sediment. Once the OCR for a cohesionless soil is known, the cone bearing resistance is first corrected for overconsolidation effects by applying the equation suggested by Schmertmann (1978):

$$q_{cOC}/q_{cNC} = 1 + 0.75\left[(OCR)^{0.42}-1\right] \qquad (4)$$

in which q_{cOC} is the cone bearing resistance registered by the cone tip from the overconsolidated cohesive sediment, and q_{cNC} is the equivalent cone bearing resistance if the same sediment were normally consolidated. q_{cNC} is then used to predict the relative density, D_r, according to fig. 6. The drained angle of friction, ϕ', can then be estimated from D_r according to figure 13.

Finally, K_0 is determined by combining the relationship proposed by Brooker and Ireland (1965) and by Schmertmann (1978):

$$K_0 = (1-\sin\phi')(OCR)^{0.42} \qquad (5)$$

As previously noted, the procedure described above does not work well with all sediment at these two stations. When a transition zone exists between layers of cohesive or cohesionless sediment and the sediment type in the transition zone is between silty sand and sandy silt, we found that the cone resistance reading for this zone has the typical response of a sand even though the friction ratio suggests the behavior of a clay or silt. Consequently, the use of Eq. (3) will result in too high an estimate for S_u, yet the cone resistance fails to predict a reasonable relative density as well. For example, layer 6-5 at depths between 30.5 and 32 m has an average f_s close to 5 kg/cm^2 with a corresponding S_u=4 kg/cm^2. This S_u would result in a S_u/σ' of 1.33 and an OCR of 6, a rather unrealistic occurence considering the corresponding values of stiff clay immediately below.

Because of the limited thickness of these transition zones and because of the depositional characteristics at these two stations, we believe that the shear strength of these layers of silty sands can be approximated by the strength of their adjacent layers. Although cementation may be a cause for sediment to have unusually high strength, we have found no evidence to support this possibility.

Results of our interpretation are given in figures 14 and 15 for the strength profiles at stations 6 and 7 respectively. In both figures, the strength for cohesive sediments are represented by S_u and marked in small circles whereas the strength for cohesionless sediments are represented

by τ_{max} and marked in solid dots. In computing τ_{max} according to Eq. (2) for cohesionless sediments, we have assumed zero cohesion.

Comparison between figures 14 and 15 indicates that the sediment at station 7 has higher strength between 10 and 20 m than equally deep sediment at station 6. Above 10 m, station 7 should be considered weaker because of the presence of sand lenses near the surface. Below 20 m, both sites can be considered as normally consolidated. The assumption of an artesian pressure head of 8 m results in an OCR of 1 for the clayey silt at 20 m. A lower artesian head would put the same clayey silt in the underconsolidated state and a higher artesian head would make the clayey silt slightly overconsolidated but would also reduce the τ_{max} value of the sand lenses. Consequently, the 8-m pressure head appears to be a logical choice.

It was noted earlier that the ground water table is near the surface and at the depth of 8 m, respectively, at stations 7 and 6, and that station 6 is moving downward relative to station 7. It follows that the overconsolidation may be attributed mainly to erosion at station 7 and desiccation at station 6.

ADDITIONAL REMARKS

We have presented field and laboratory data for stations 6 and 7 and described our attempt to show the type and the extent of information on sediment parameters that can be established from these data for the purpose of conducting seismic response analyses. In carrying out this exercise we are convinced that while cone penetration test alone may be adequate for settlement prediction and pile design, additional laboratory work is definitely needed to supplement CPT results for seismic studies. Although we have demonstrated that shear strength can be interpreted from penetration tests, there are not sufficient laboratory data to allow us to calibrate the

cone results and to assess the applicability of the empirical relations we used.

Since the downhole seismic survey directly measures the seismic motion in situ, this method provides the most reliable values of G_{max}. It should be noted, however, that the method based on the average value over a fixed interval does not provide the fine details on local variation in sediment properties as can be obtained with the continuous CPT. A compromise has to be made in applying these field data to decide what extent of local variation in soil properties is meaningful and should be considered.

In reviewing the procedure for estimating the shear strength, we feel that the most crucial assumptions made were to treat the ratio, S_u/σ_v' as 0.33 for clays with OCR=1 and the validity of figure 12. The OCR resulting from these assumptions serves as a reference from which the past loading history at a site is derived. Consequently, any deviation from the 0.33 value or the plot in figure 12 may have a substantial effect on our estimates of τ_{max}. If and when the opportunity arises, we strongly recommend that consolidation or triaxial tests be performed on undisturbed samples from selected cohesive sediments at these two stations. Groundwater conditions at these two stations also merit confirmation.

Finally, we wish to stress that the strength profiles presented in figures 14 and 15 only represented our best estimates from presently available geotechnical data at these two sites. These strength profiles are subject to further modifications when additional information from the two sites becomes available. For example, an ongoing field investigation indicates that the artesian pressure at station 6 may not have originated from the sand layer at 8-15 m but rather from the layer at 25-29 m. If this proves to be true estimates of shear strength at station 6 have to be revised accordingly based

on a totally different vertical effective stress profile. Nevertheless, we believe that the procedure described is a logical one and that the report is useful in planning and executing further geotechnical investigations of similar nature. If the readers are convinced that additional laboratory works are necessary for this type of investigation, the report would have served its purpose.

ACKNOWLEDGEMENTS

We thank R. L. Porcella, USGS, for providing us with the wave velocity profiles at stations 6 and 7, and Elizabeth Turner, Univeristy of Texas at Austin, for sharing with us some yet-to-be-published laboratory results. Homa Lee and Les Youd, both at USGS, reviewed the report and offered many constructive suggestions.

REFERENCES CITED

ASTM Standards. Part 19, 1978, Natural building stones; soil and rock, peats, mosses and humus: American Society fo Testing and Materials, Philadelphia, Pennsylvannia

Brooker, E. W., and Ireland, H. O., 1965, Earthpressures at rest related to stress history: Canadian Geotechnical Journal, Vol. 11, No. 1, February, pp. 1-15.

Casagrande, Arthur, 1948, Classification and identification of soils: Transactions, American Society of Civil Engineers, v. 113, p. 919-922.

Elders, W.A., 1979, The geological background of the geothermal fields of the Salton trough, in Elders, W.A., ed., Geology and geothermics of the Salton trough: Geological Society of America, 92nd Annual Meeting, San Diego, California, Guidebook for field trip no. 7, and University of California, Riverside, Campus Museum Contributions no. 5, p. 1-19

Drnevich, V. P., Gorman, C. T., and Hopkins, T. C., 1974, Shear strength of cohesive soils and friction sleeve resistance: Proceedings, European Symposium on Penetration Testing, Stockholm, Vol. 1, pp. 129-132.

Fumal, T.E., Gibbs, J.F., and Roth, E.F., 1982, In-situ measurements of seismic velocity at 10 strong motion accelerograph stations in central California: U.S. Geological Survey Open File Report 82-407, 76 p.

Hardin, B. O., and Drnevich, V. P., 1972, Shear modulus and damping -- design equations and curves: Journal of the Soil Mechanics and Foundation Division, ASCE, Vol. 98, No. SM7, July, pp. 667-692.

Kobayashi, N., 1959, A method of determing the underground structure by means of SH waves: Zisin, ser. 2, v. 12, p. 19-24.

Lambe, T.W., and Whitman, R.V., 1969, Soil Mechanics: New York, John Wiley and Sons, 533 p.

Martin, G.R., and Douglas, B.J., 1981, Evaluation of the cone penetrometer for liquefaction hazard assessment: U.S. Geological Survey Open File Report 81-284, 359 p.

Mendenhall, W.C., 1909, Groundwater of the Indio region, California: U.S. Geological Survey Water-Supply Paper 225, 56 p.

Muller, C. S., Boore, D. M., and Porcella, R. L., 1982, Detailed study of site amplification at El Centro Strong-Motion Array Station #6: Proceedings, 3rd International Earthquake Microzonation Conference, June 28-July 1, 1982, Seattle, U.S.A., Vol. 1, pp. 413-424.

Sanglerat, G., 1972, The Penetrometer and Soil Exploration: Elsevier Publishing Co., New York, 434 p.

Schmertmann, J.H., 1978, Guidelines for cone penetration test, performance and design: U.S. Department of Transportation, Federal Highway Administration, FHWA-TS-78-209, 143 p.

Seed, H.B., Woodward, R.J., and Lundgren, Richard, 1964, Clay mineralogical aspects of the Atterberg limits: Journal of Soil Mechanics Division, v. 90, p. 107-131.

Sharp, R.V., 1972, Tectonic setting of the Salton Trough, in, The Borrego Mountain earthquake of April 9, 1968: U.S. Geological Survey Professional Paper, 787, p.3-15

Shepard, F.P., 1954, Nomenclature based on sand-silt-clay ratios: Journal of Sedimentary Petrology, v. 24, p. 151-158

Skempton, A. W., 1944, Notes on the compressibility of clayes: Geological Society of London Quaterly Journal, v. 50, p. 119-135.

Terzaghi, K., and Peck, R.B., 1967, Soil Mechanics in Engineering Practice: 2nd ed., John Wiley and Sons, Inc., New York, 729 p.

Van De Kamp, P.C., 1973, Holocene continental sedimentation in the Salton Basin, California; a Reconnaissance: Geological Society of America Bulletin, v. 84, no. 3, p. 827-848

Warrick, R.E., 1974, Seismic investigation of a San Francisco Bay mud site: Bulletin of the Seismological Society of America, v. 64, p. 375-385.

Youd, T.L., and Wieczorek, G.F., in press, Liquefaction and secondary ground failure: in U.S. Geological Survey Professional Paper 1254.

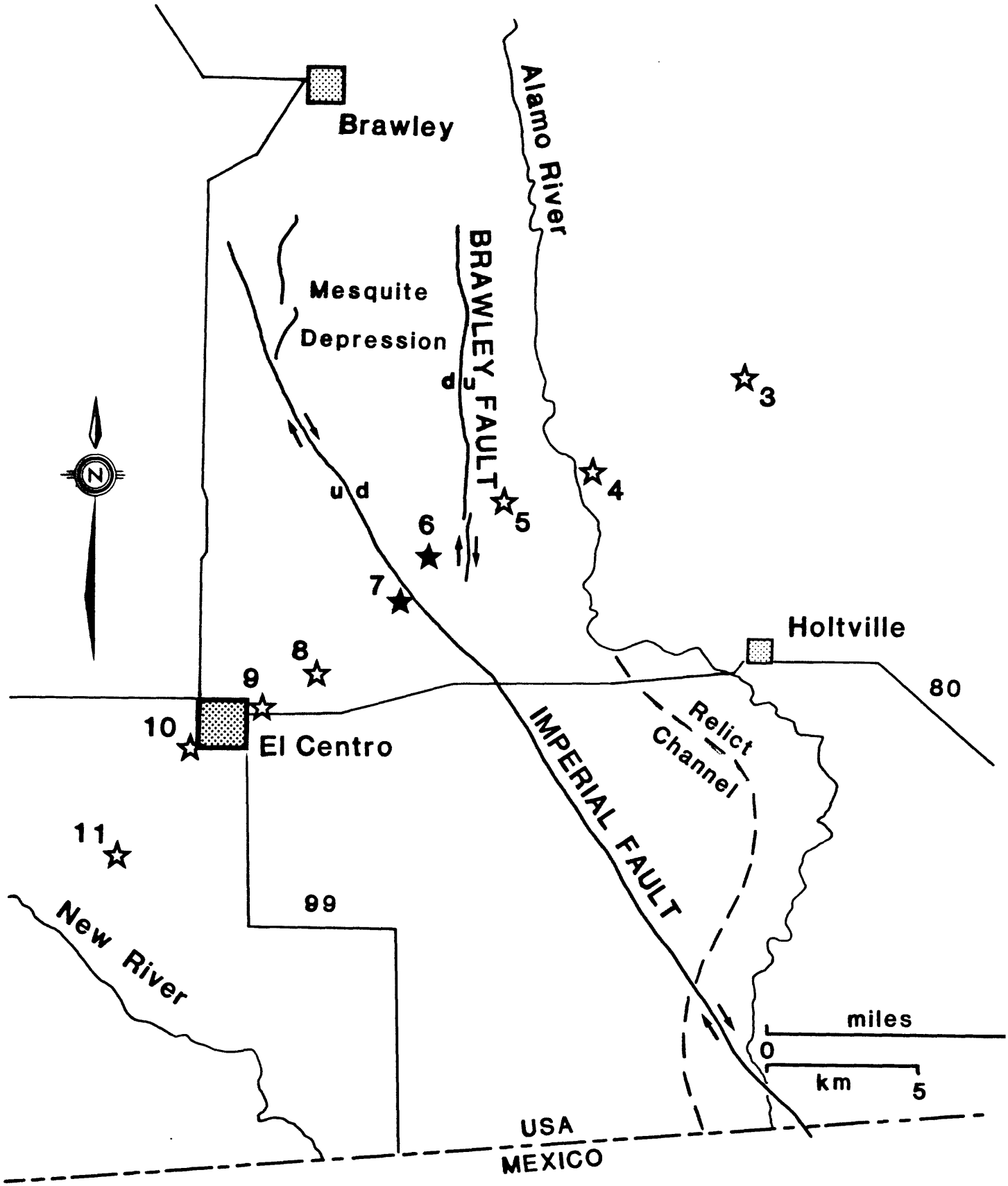

Figure 1. Location of strong motion stations.

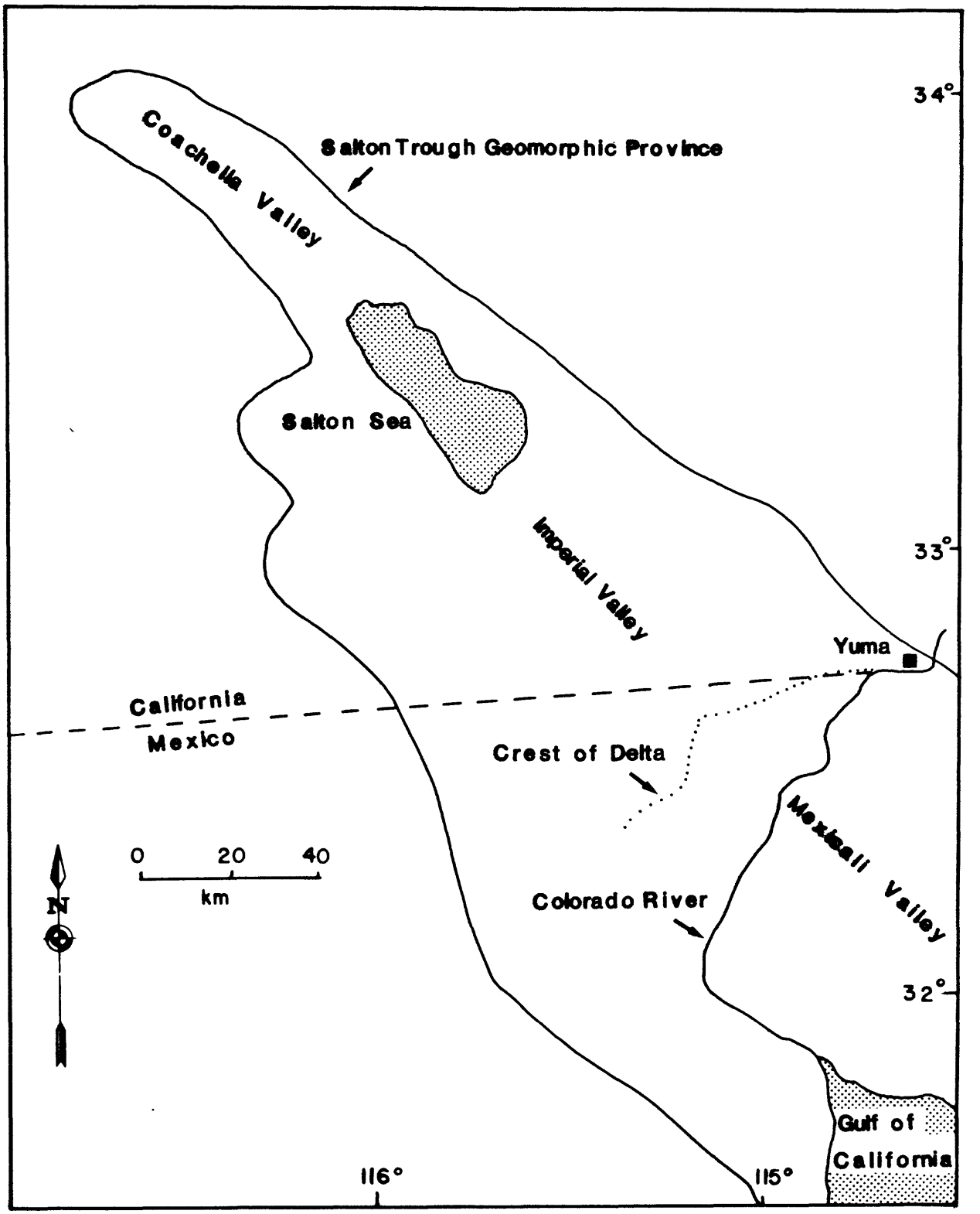

Figure 2. Geographic features of the Imperial Valley region.

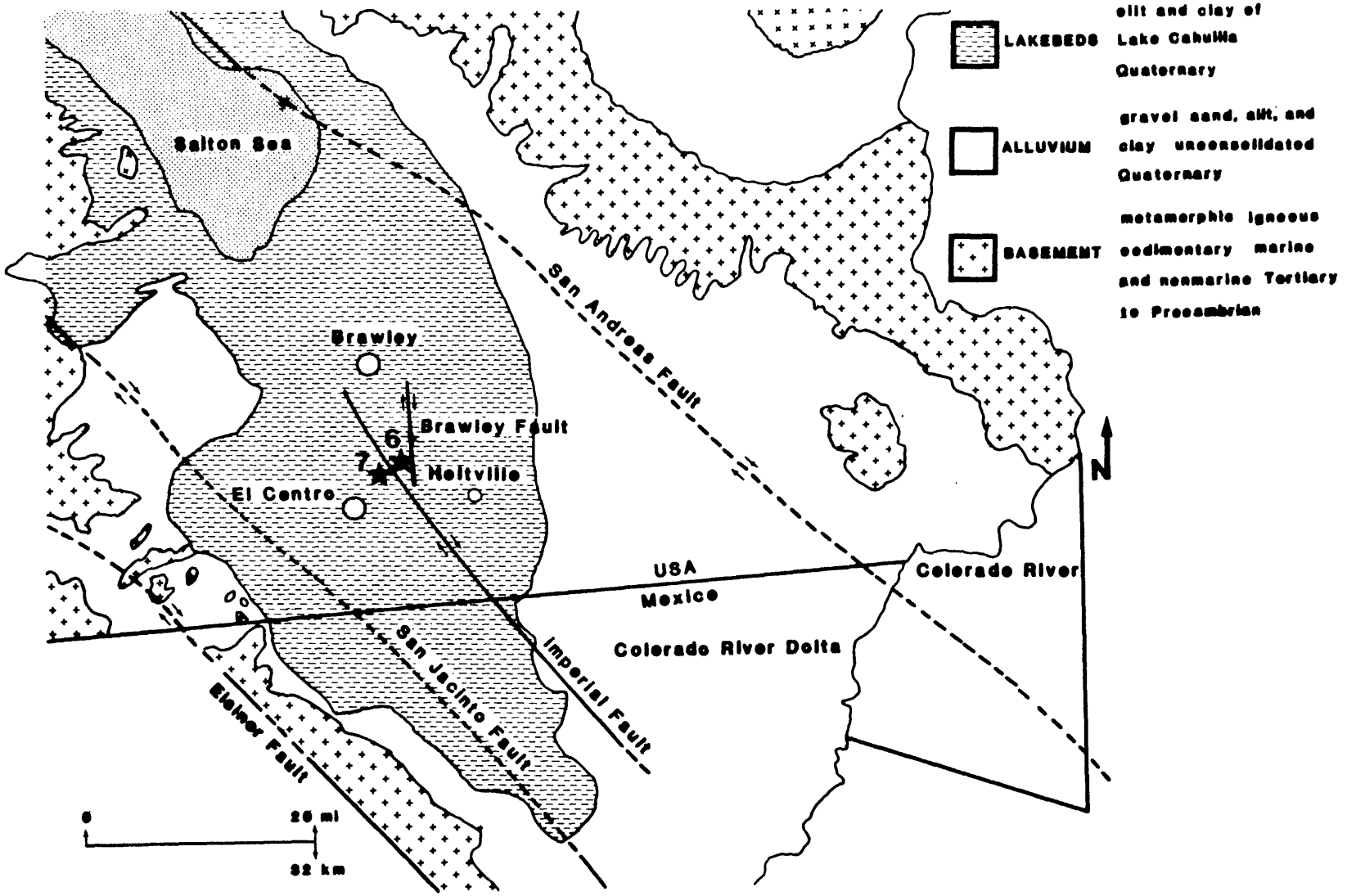

Figure 3. Generalized geologic map of Imperial Valley region.

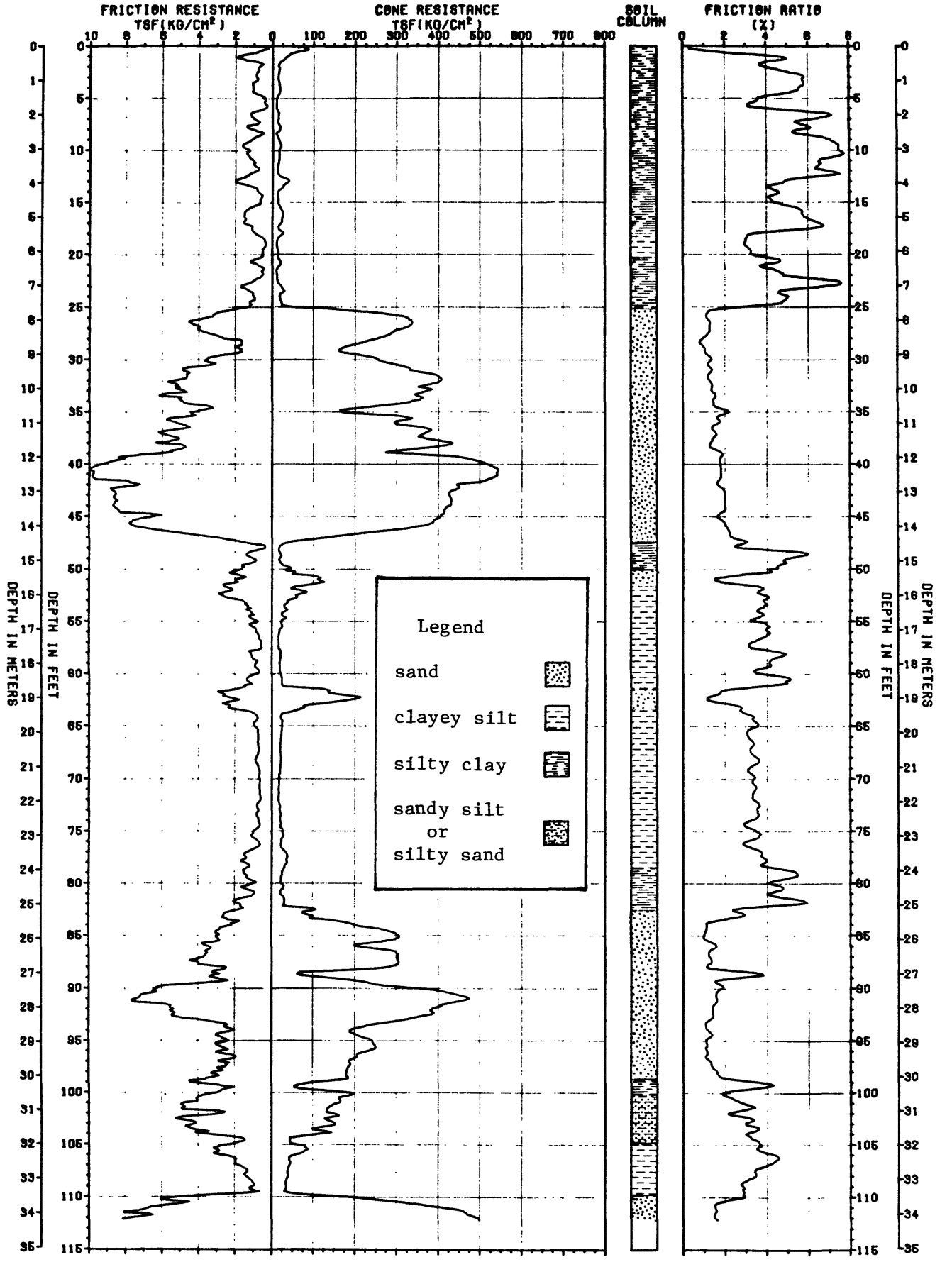

Figure 4. Log of station 6.

Cone resistance scale changed to 800

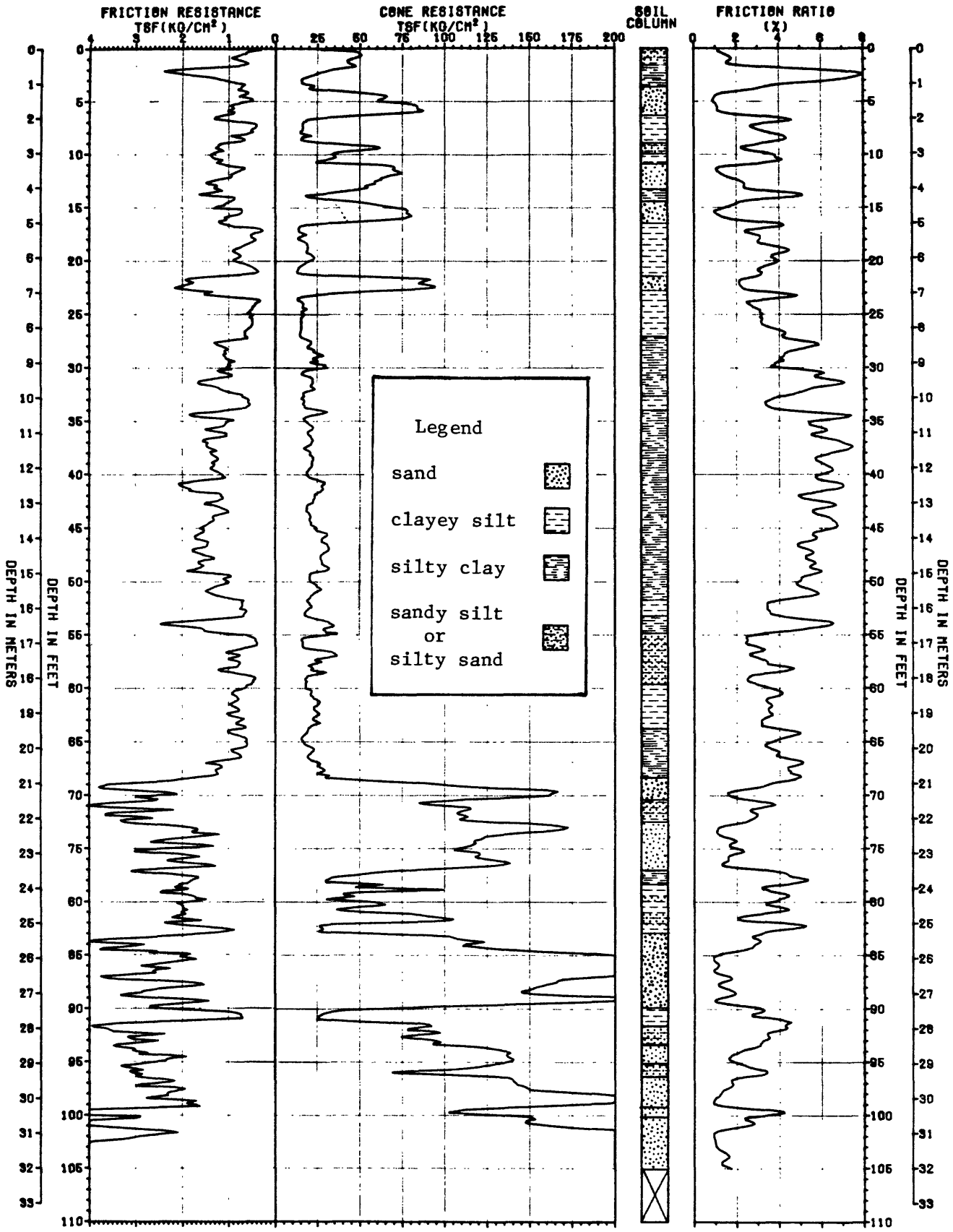

Figure 5. Log of station 7.

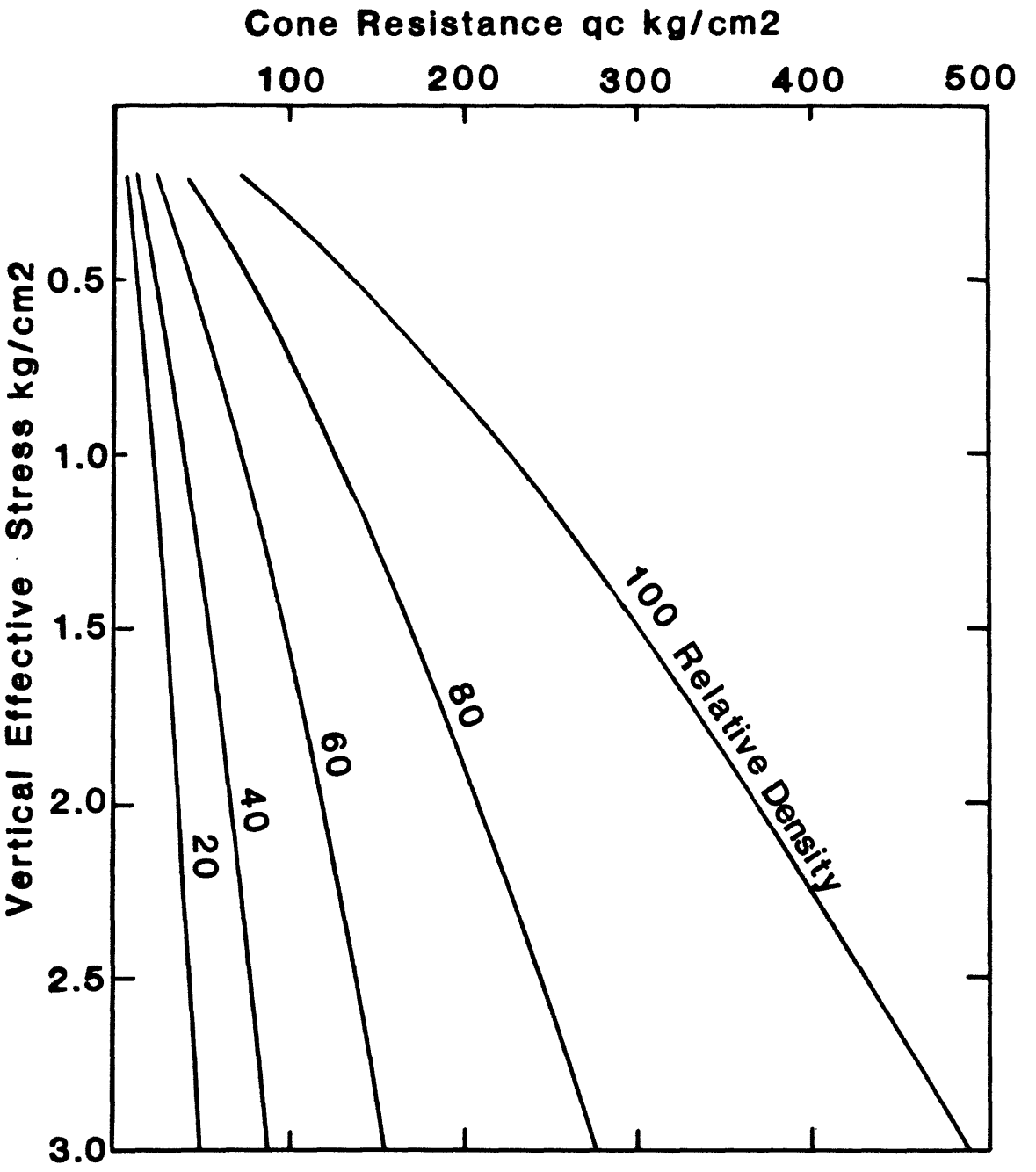

Figure 6. Relative density determined from CPT and vertical effective stress (Schmertmann, 1978).

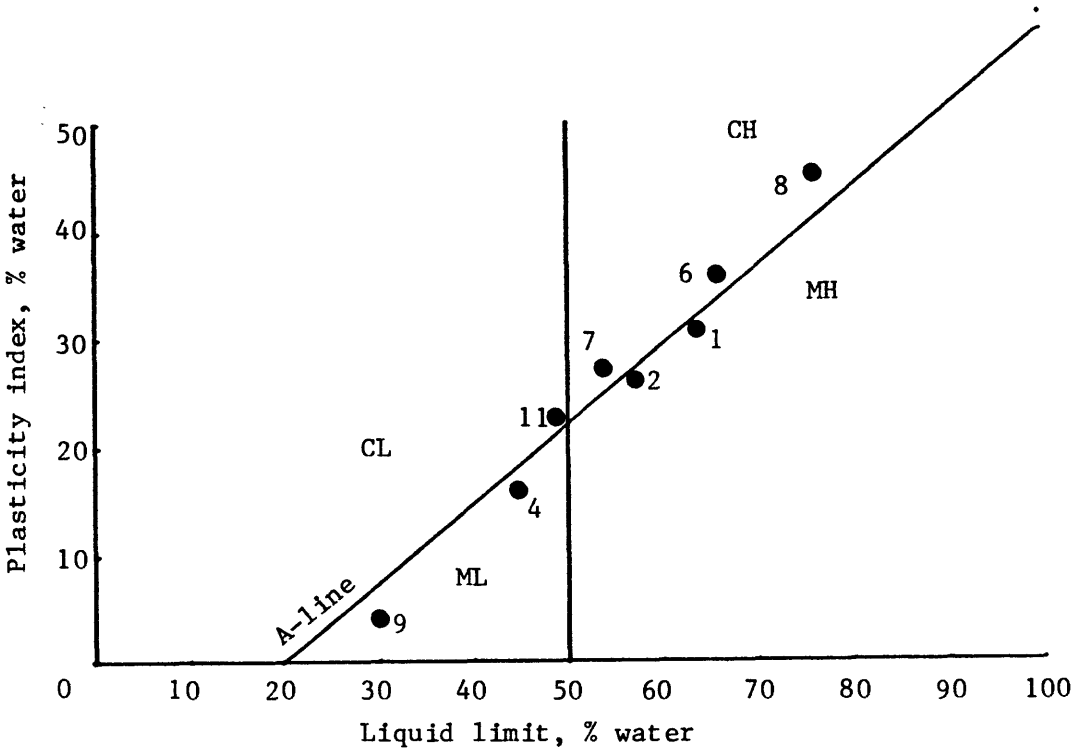

Figure 7. Unified soil classification of fine sediment

no.	hole/depth m
1	6/2.7
2	6/6.9
3	6/11.6
4	6/14.3
5	6/22.1
6	6/29.0
7	7/2.7
8	7/13.7
9	7/22.9
10	7/26.5
11	7/26.5

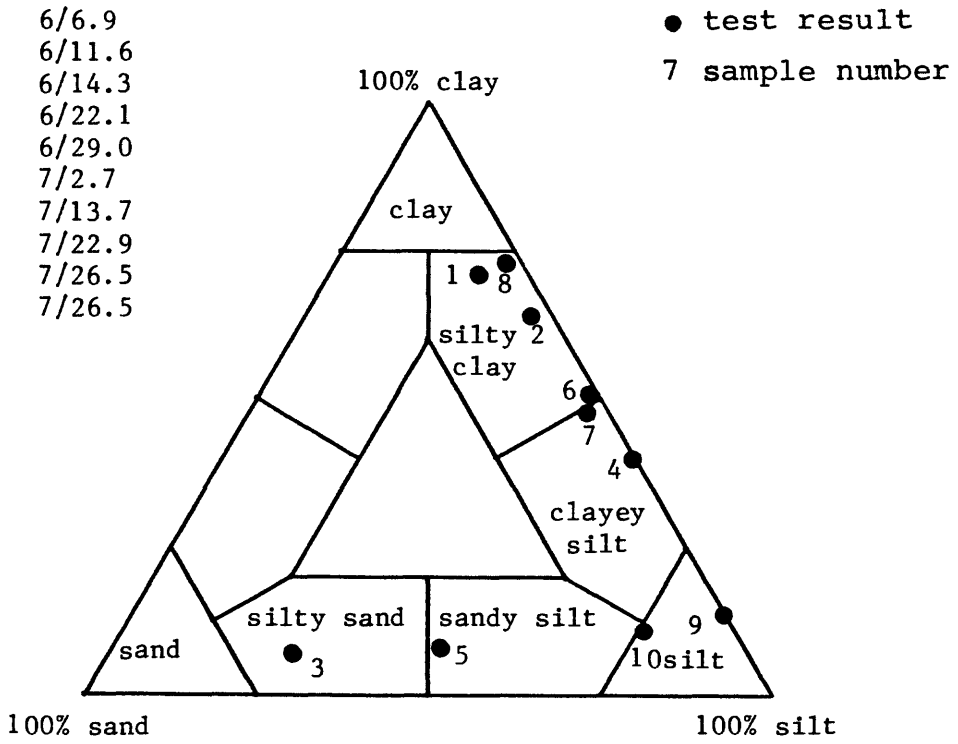

Figure 8. Shepard classification of sediment.

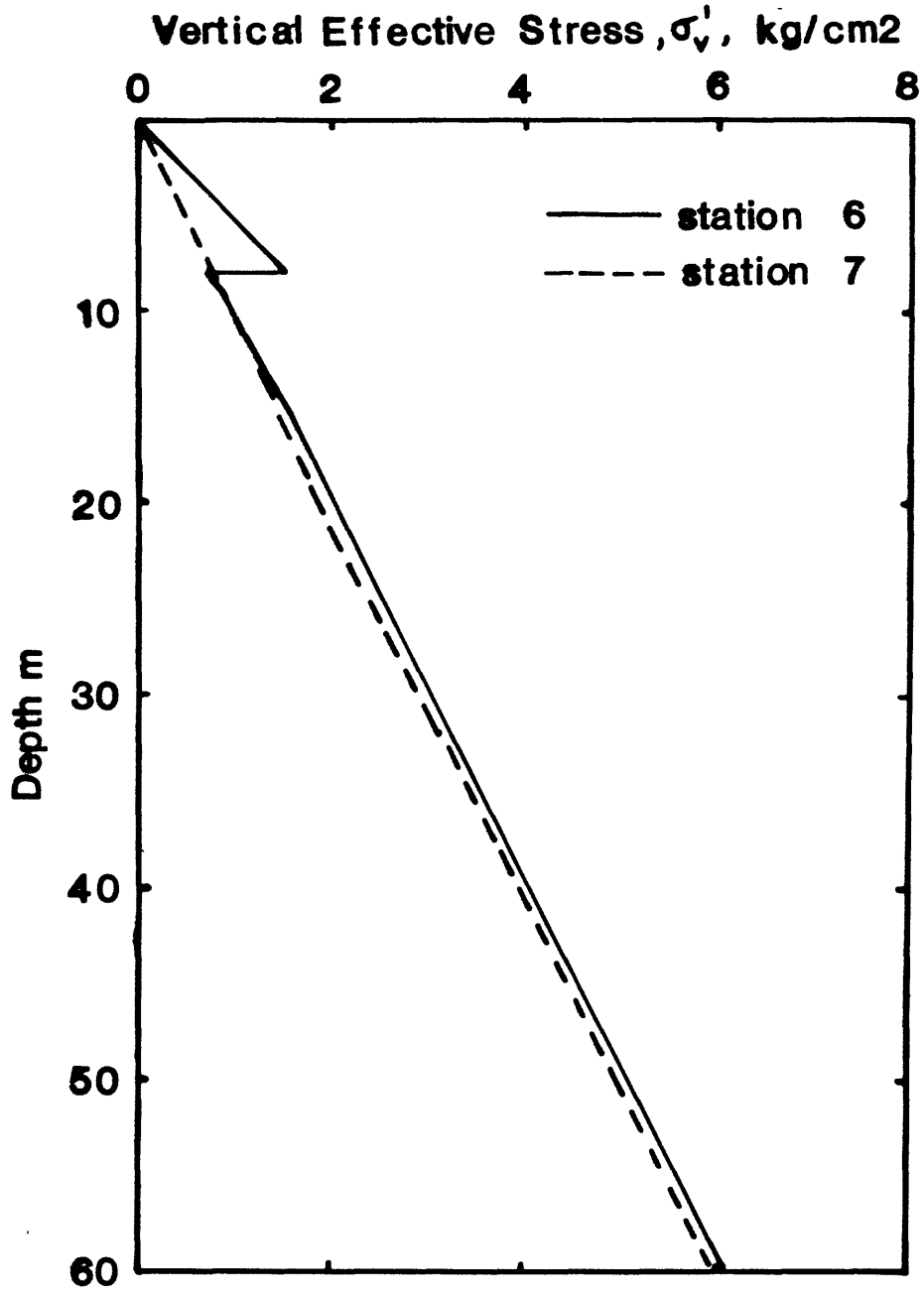

Figure 9. Vertical effective stress versus depth at stations 6 and 7.

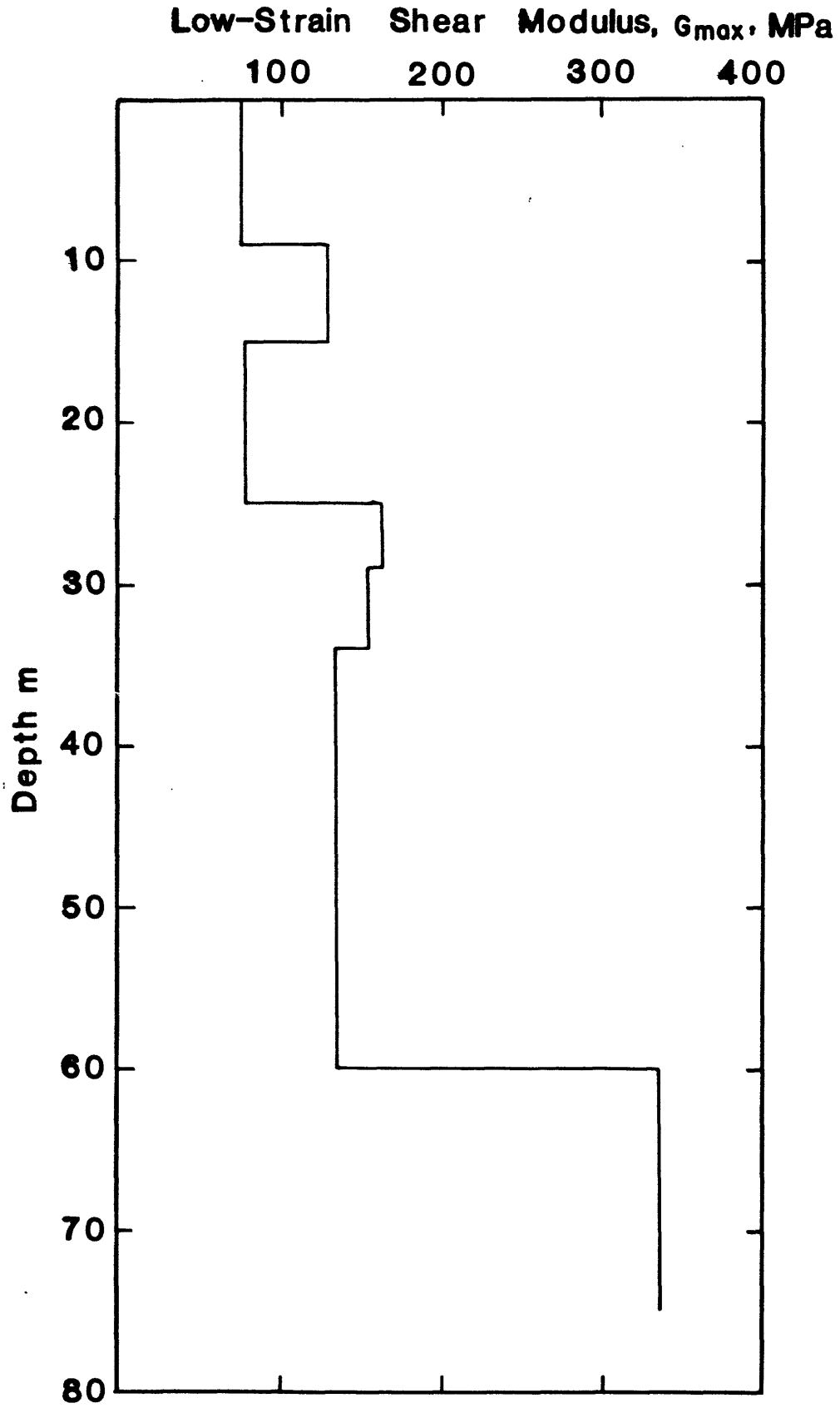

Figure 10. Low-strain shear modulus versus depth at station 6.

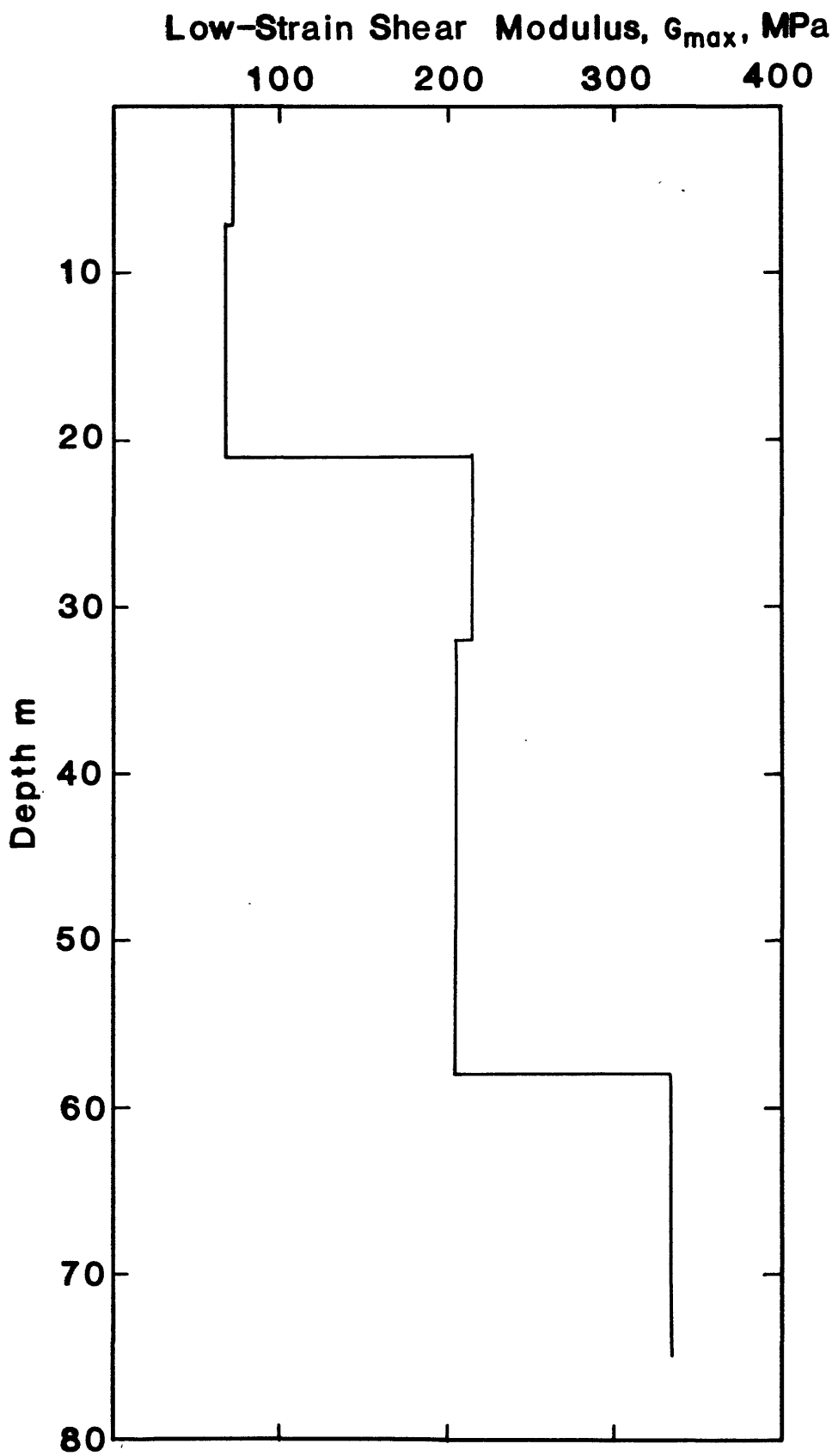

Figure 11. Low-strain shear modulus versus depth at station 7.

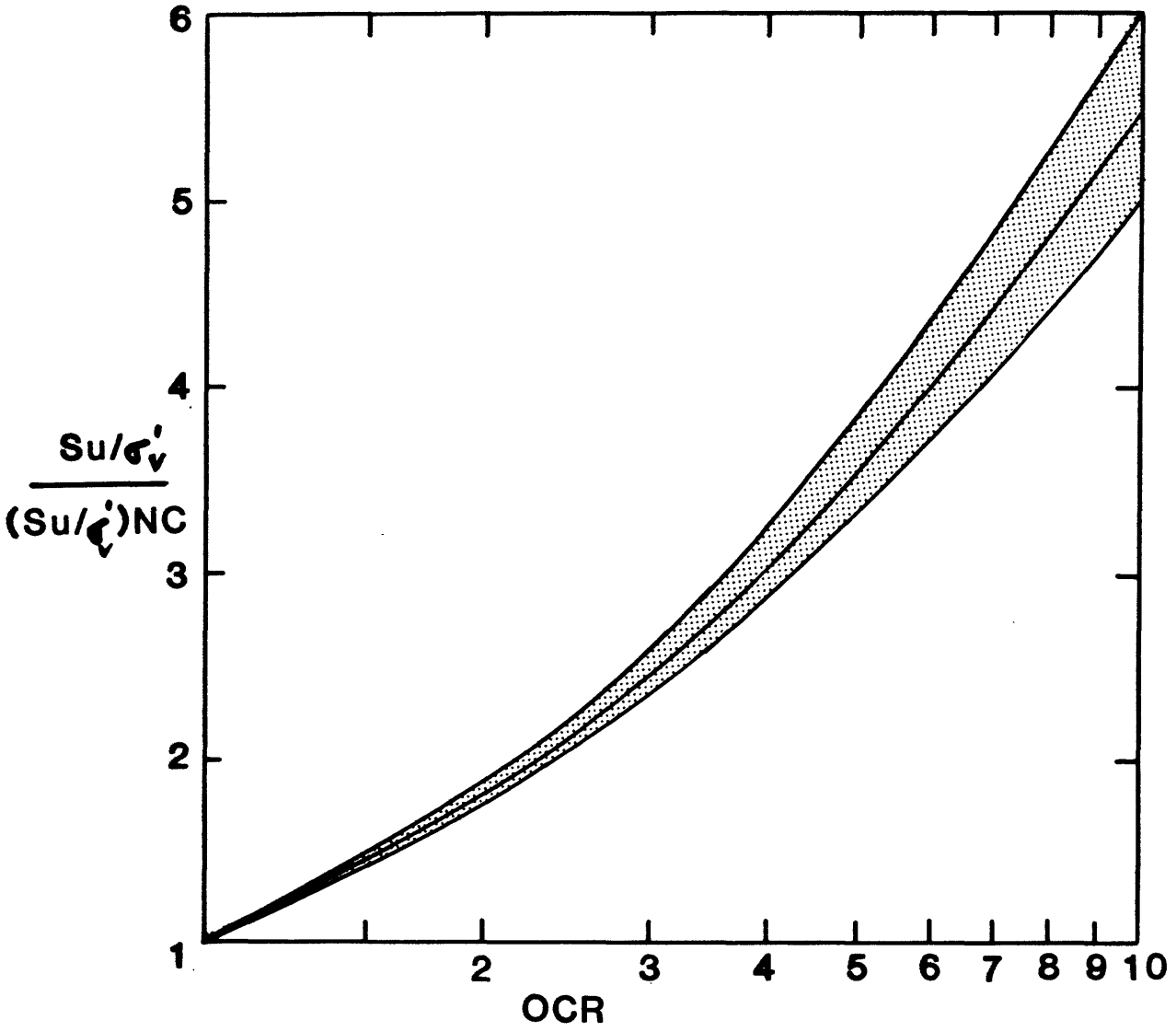

Figure 12. Normalized (Su/σ_v') ratio versus OCR (Schmertmann, 1978).

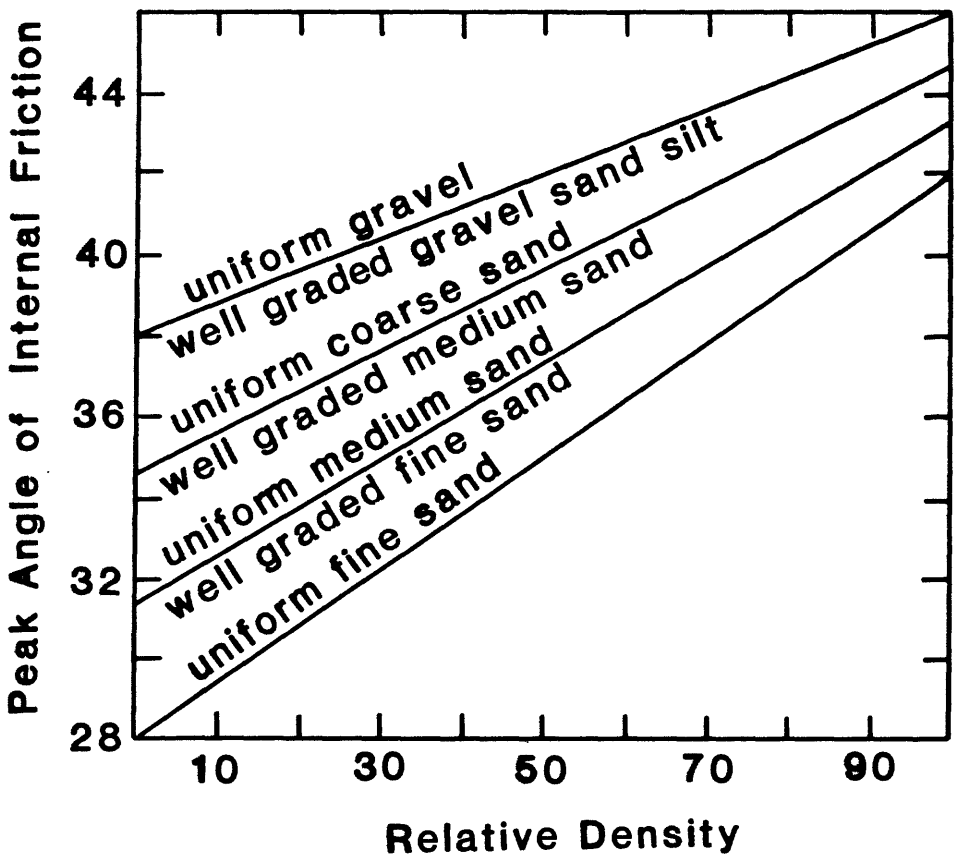

Figure 13. Friction angle versus relative density (Schmertmann, 1978).

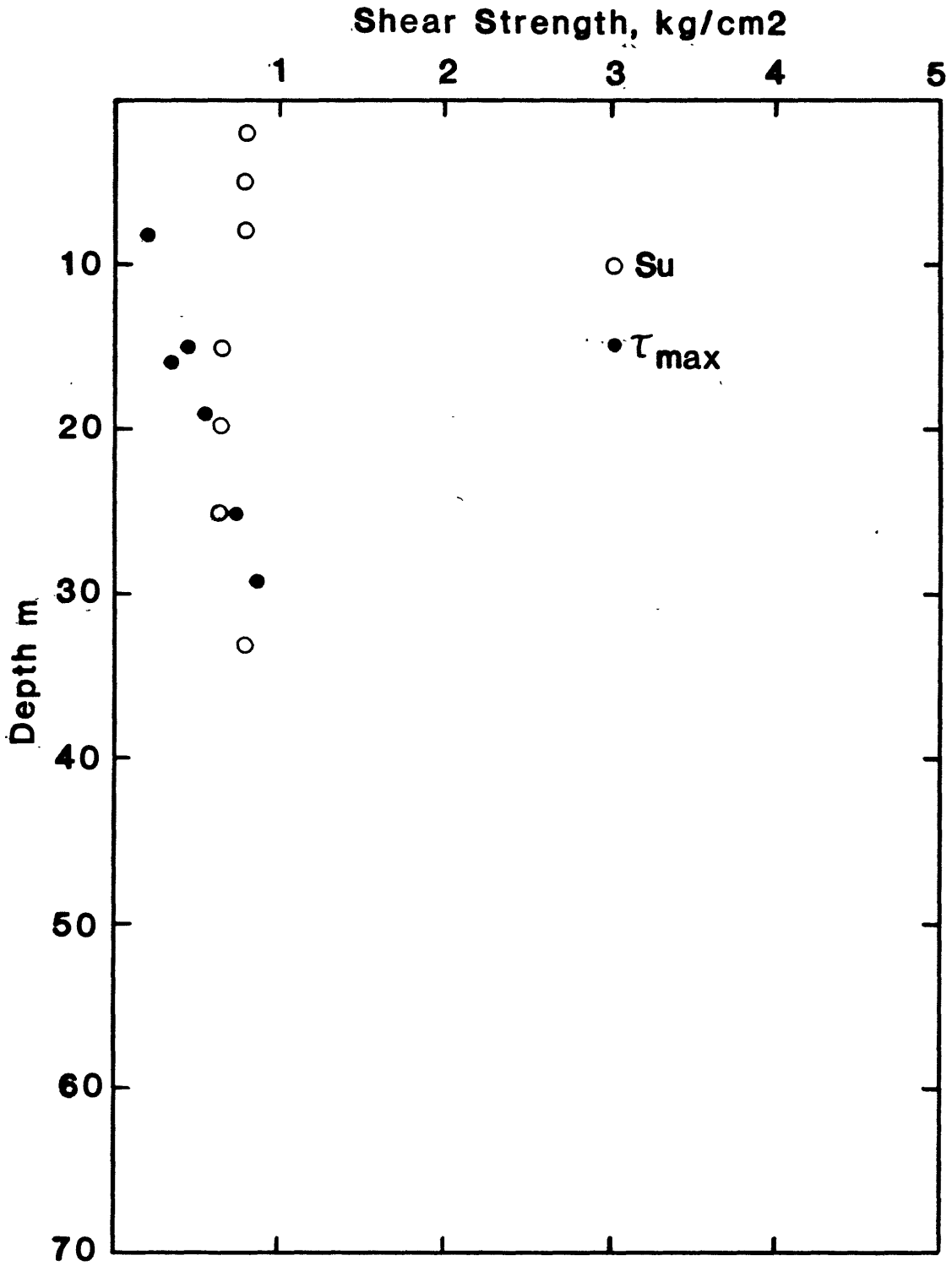

Figure 14. Estimated shear strength profile at station 6.

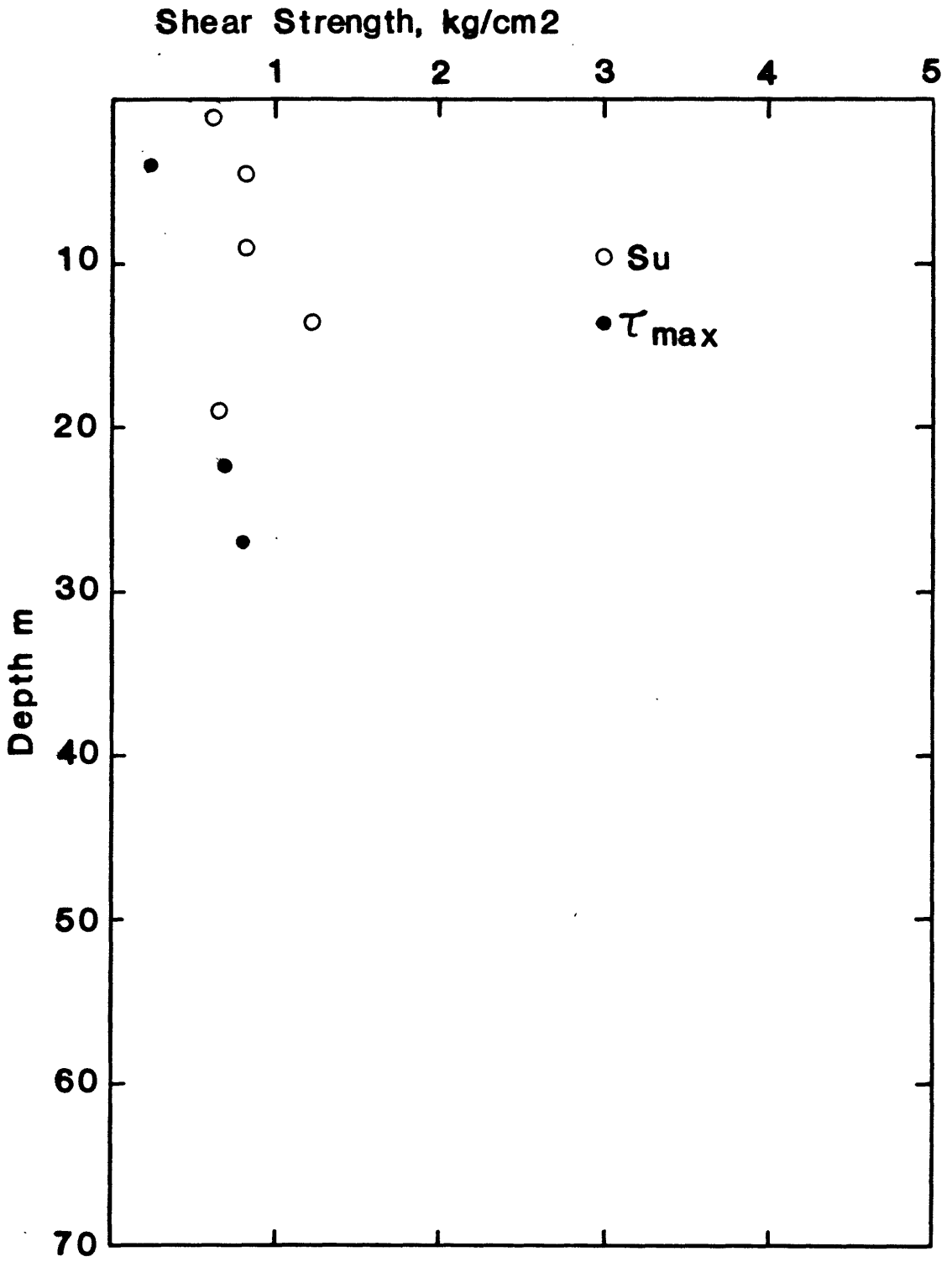

Figure 15. Estimated shear strength profile at station 7.

Table 1. Sediment description of stations 6 and 7

Soil Layer No.	Sample Depth m	Sand	Silt	Clay	W_n	W_l	W_p	D_{50}	Bulk Density	SPT N	Strength kg/cm^2
6/1	2.7	7	22	71	28	64	33	.001	x	16	x
6/1	2.8	x	x	x	32	x	x	x	1.93	x	0.94
6/1	3.4	x	x	x	30	x	x	x	1.96	x	0.86
6/1	6.9	3	33	64	x	57	31	.002	x	x	x
6/2	11.6	66	27	7	x	x	x	.080	x	50+	x
6/2	14.3	0	60	40	x	45	29	.006	x	x	x
6/3	22.1	44	48	8	x	x	x	.056	x	x	x
6/5	29.0	1	48	51	28	66	30	.004	x	43	x
7/1	2.7	3	49	48	31	54	27	.004	x	10	x
7/2	13.7	2	25	73	x	76	31	.001	x	x	x
7/3	22.9	0	86	14	31	30	26	.014	x	48	x
7/3	26.5	13	76	11	x	x	x	.027	x	x	x
7/3	26.5	x	x	x	31	49	26	x	x	x	x

W_n = natural water content, W_l = liquid limit, W_p = plastic limit, D_{50} = median grain size, N = blows/foot

Table 2 -- Site Description of Station 6

Soil Layer No.	Description	Depth Occupied	Estimated Ave. Bulk Density in gm/cc	Ave. Shear Wave Velocity in m/s	Remarks
6-1	Medium stiff silty clay	0-8 m	1.95	200	Density averaged from samples at 2.5-4m. Ave. S_u=0.9 kg/cm^2 from same samples.
6-2	Very dense sand to silty sand	8-15 m	2.1	250	Estimated D_r=90%, an artesian pressure head of 8 m is assumed.
6-3	medium stiff clayey and dense sand	15-25 m	2.0	200	Dense sand lenses at 16 and 19 m with estimated D_r of 70 & 80%.
6-4	Very dense sand	25-29 m	2.1	280	Estimated D_r=85%
6-5	dense silty sand and stiff clay.	29-34 m	2.0	280	
6-6	medium to stiff clay some coarse sand	34-60 m		260	CPT stopped at 34 m.
6-7	medium stiff clay some fine sand	60-75 m		400	

Table 3 -- Site Description of Station 7

Soil Layer No.	Description	Depth Occupied	Estimated Ave. Bulk Density in gm/cc	Ave. Shear Wave Velocity in m/s	Remarks
7-1	Interbeded med dense sand and med stiff clayey silt	0-7 m	2.0	190	Ground water table at the surface. Estimated D_r=78% for sand at 4 m.
7-2	Med stiff to stiff clayey silt, silty clay, and sandy clay	7-21 m	1.9	190	Density from samples at at 14 m.
7-3	Interbed of dense sand and stiff clayey silt	21-32 m	2.1	320	Sand lenses at 22, 27, and 30^m with eatimated D_r of 67,70, and 70%.
7-4	Assortment of dense sand, sandy and silty clay	32-58 m	2.0	320	CPT stopped at 32 m.
7-5	Assortment of sandy and silty clay	58-75 m		400	